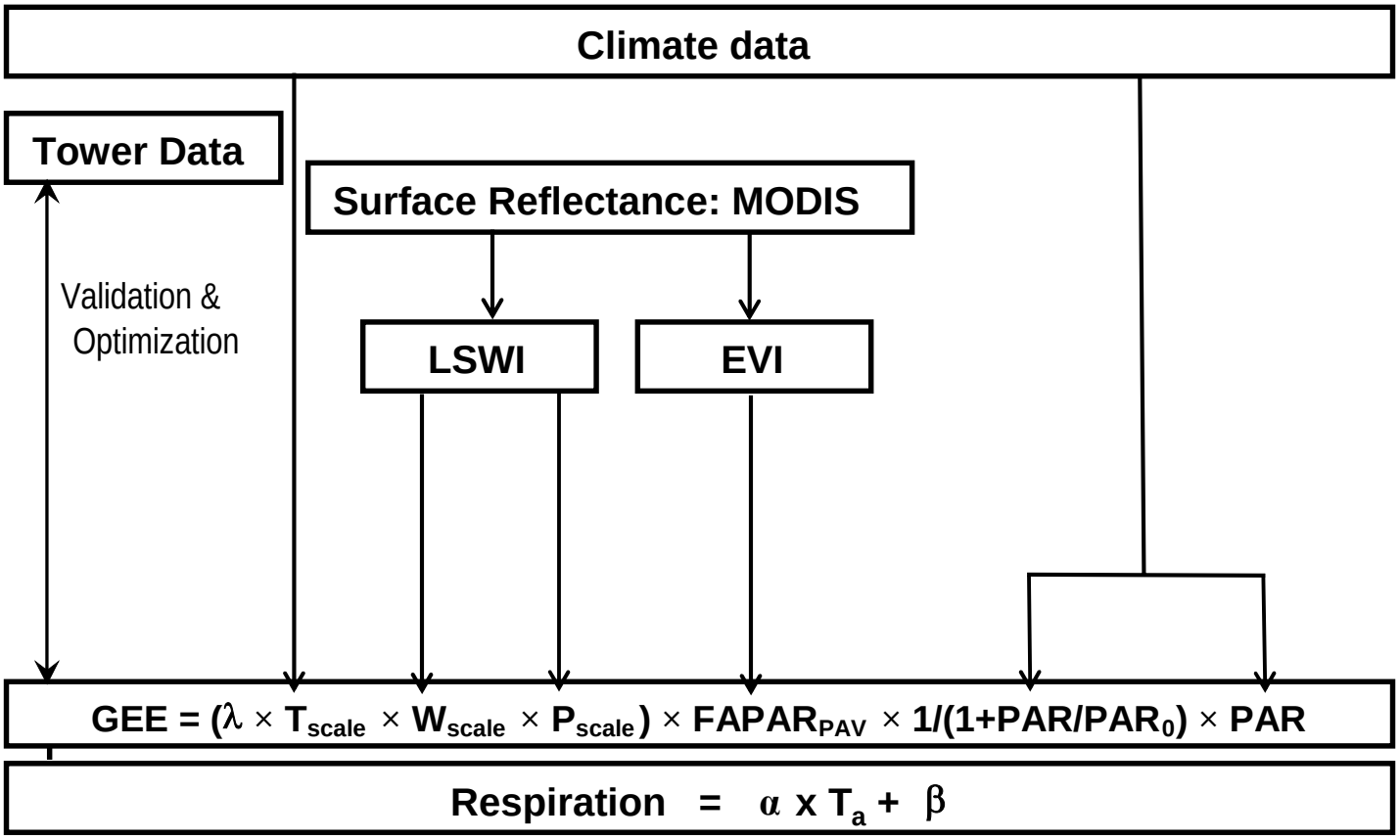


Figure 1: Schematic diagram of the Vegetation Photosynthesis Respiration Model (VPRM). EVI denotes Enhanced Vegetation Index, LSWI-Land Surface Water Index; $FPAR_{PAV}$-the fraction of incident light absorbed by the photosynthetically active vegetation in the canopy; $T_{scale}$, $P_{scale}$ and $W_{scale}$-scalars for temperature, leaf phenology and canopy water content, respectively. GEE (Gross Ecosystem Exchange) is the light-dependent part of Net Ecosystem Exchange, R (Respiration) is the light-independent part. MODIS refers to the Moderate Resolution Imaging Spectroradiometer onboard the NASA Terra and Aqua satellites; $PAR_0$, $\lambda$, $\alpha$ and $\beta$ are the four model parameters, one set per vegetation type.

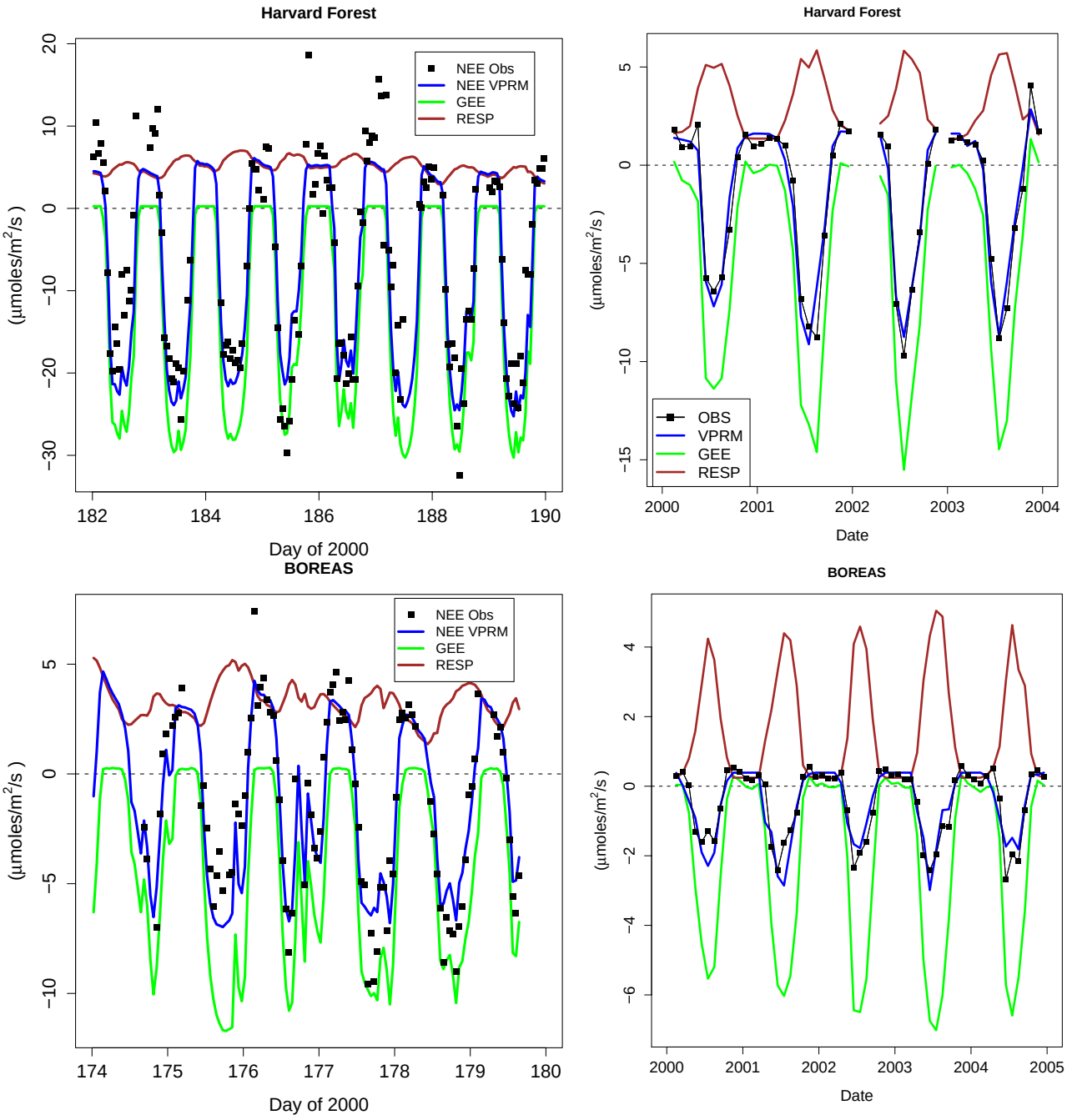


Figure 2a: (*left panels*) Examples of hourly output from the VPRM for Harvard Forest (upper) and NOBS (*lower*). Observations (points) show u*-filtered hourly data only. (*right panels*) Comparison between the observed (solid-square) and VPRM (blue line) monthly mean NEE (µmole $m^{-2}$ $s^{-1}$) over the four-year period at these two calibration sites. The VPRM provides a consistent separation of the light-dependent part of NEE ("GEE") from the light-independent part (Respiration) across all sites.

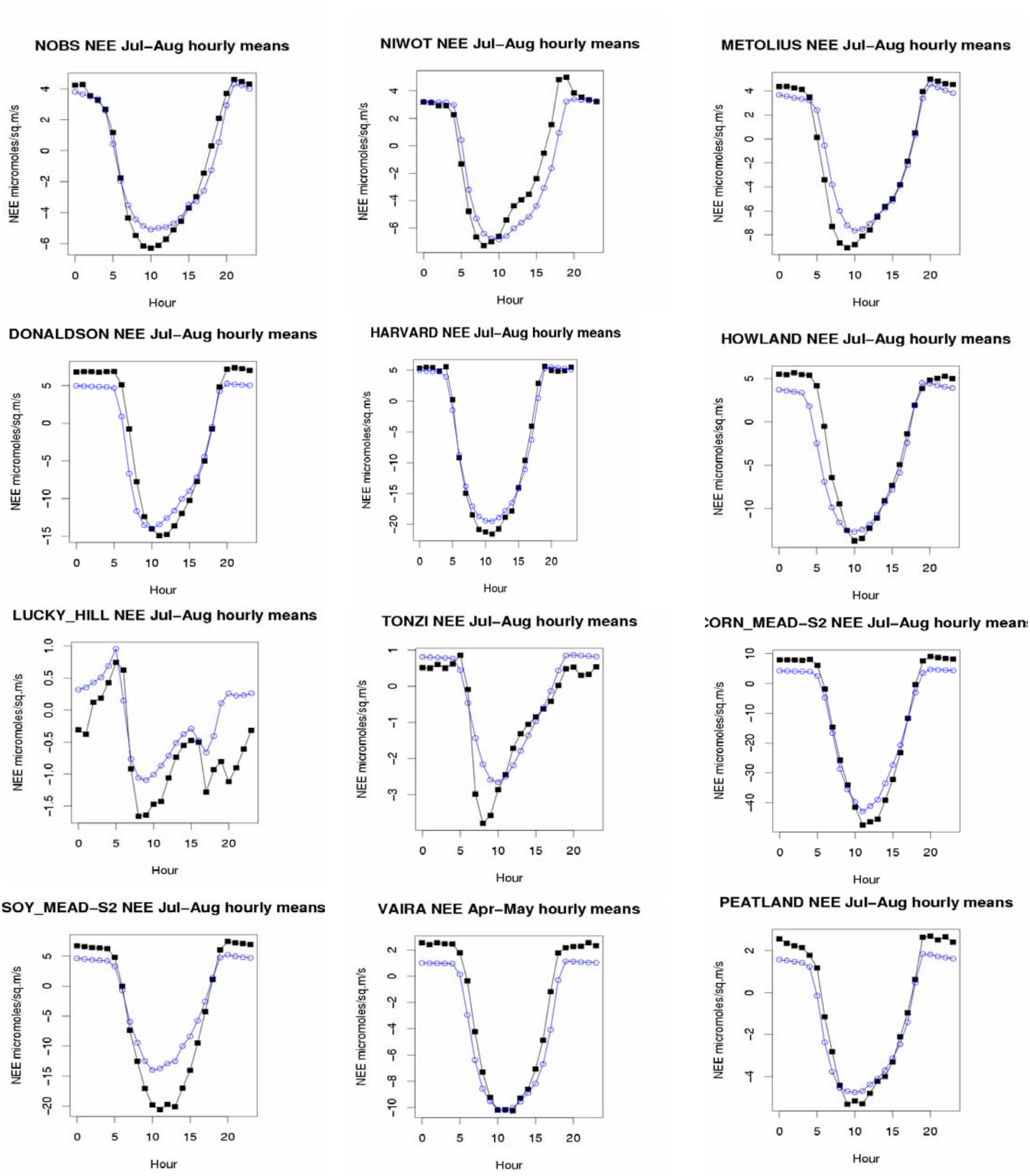


Figure 2b: A comparison between the observed (solid-square) and VPRM (open-circle) mean diurnal diurnal variation of NEE (μmole $m^{-2}$ $s^{-1}$) during the peak growing season at Calibration sites.

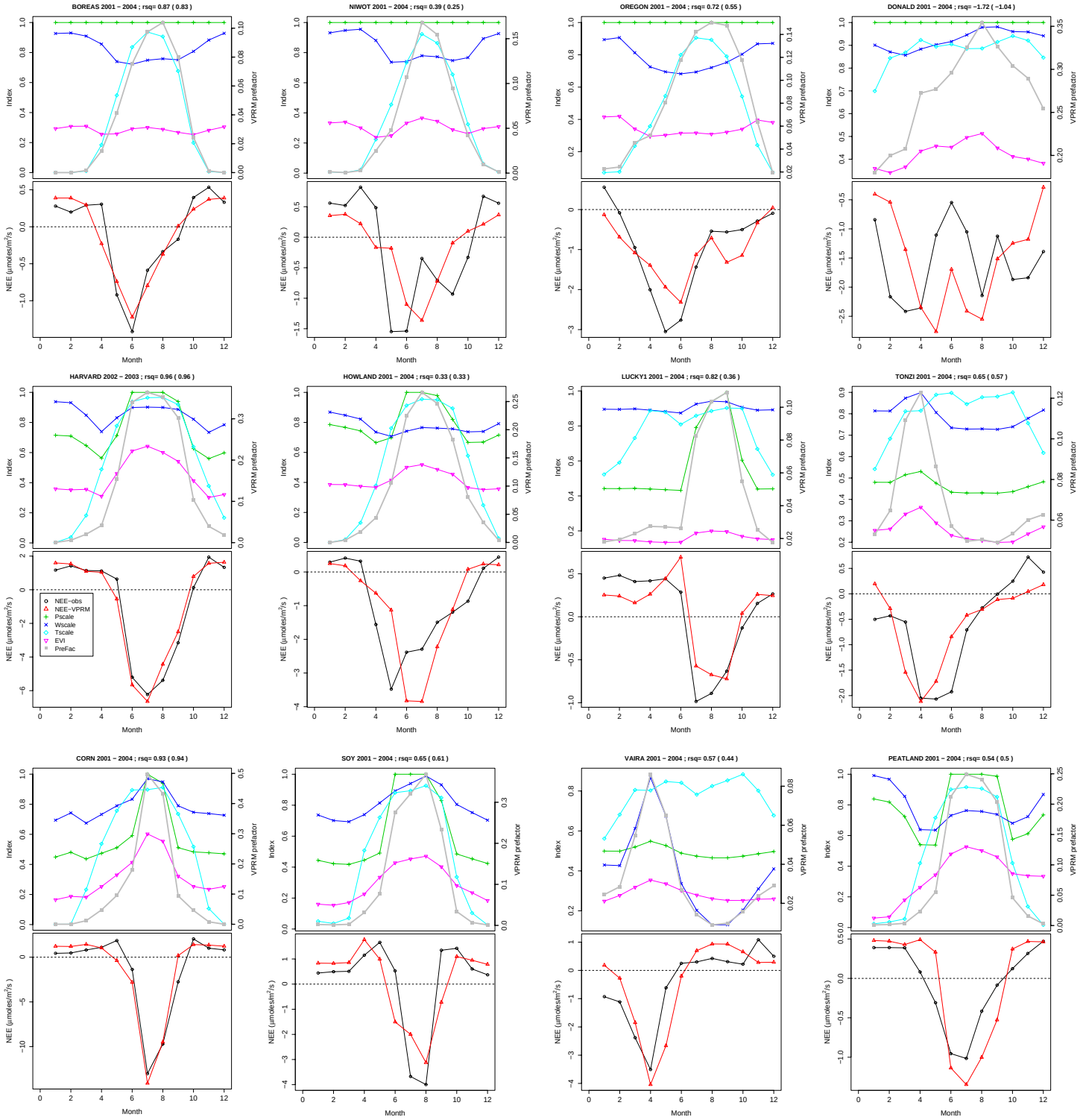


Figure 3: (*upper sections*) Seasonal dynamics of the pre-factors $T_{scale}$, $P_{scale}$, and $W_{scale}$ in the VPRM equation (Eq. 12), driven by satellite and meteorological data. All factors are significant, at various times and places. (*lower sections*) Comparison of the seasonal dynamics between observed (black) and VPRM (red) monthly mean NEE (μmole $m^{-2}$ $s^{-1}$) at calibration sites, monthly means , averaged over all years. Values in the title bar give the fraction of the total variance of the mean seasonal cycle of NEE captured by the model, [1 – var( $NEE_{obs}$ – $NEE_{VPRM}$)/var( $NEE_{obs}$)] (in parenthesis, the same quantity for the time series of individual monthly means). Note that net uptake of $CO_2$ corresponds to negative values of NEE.

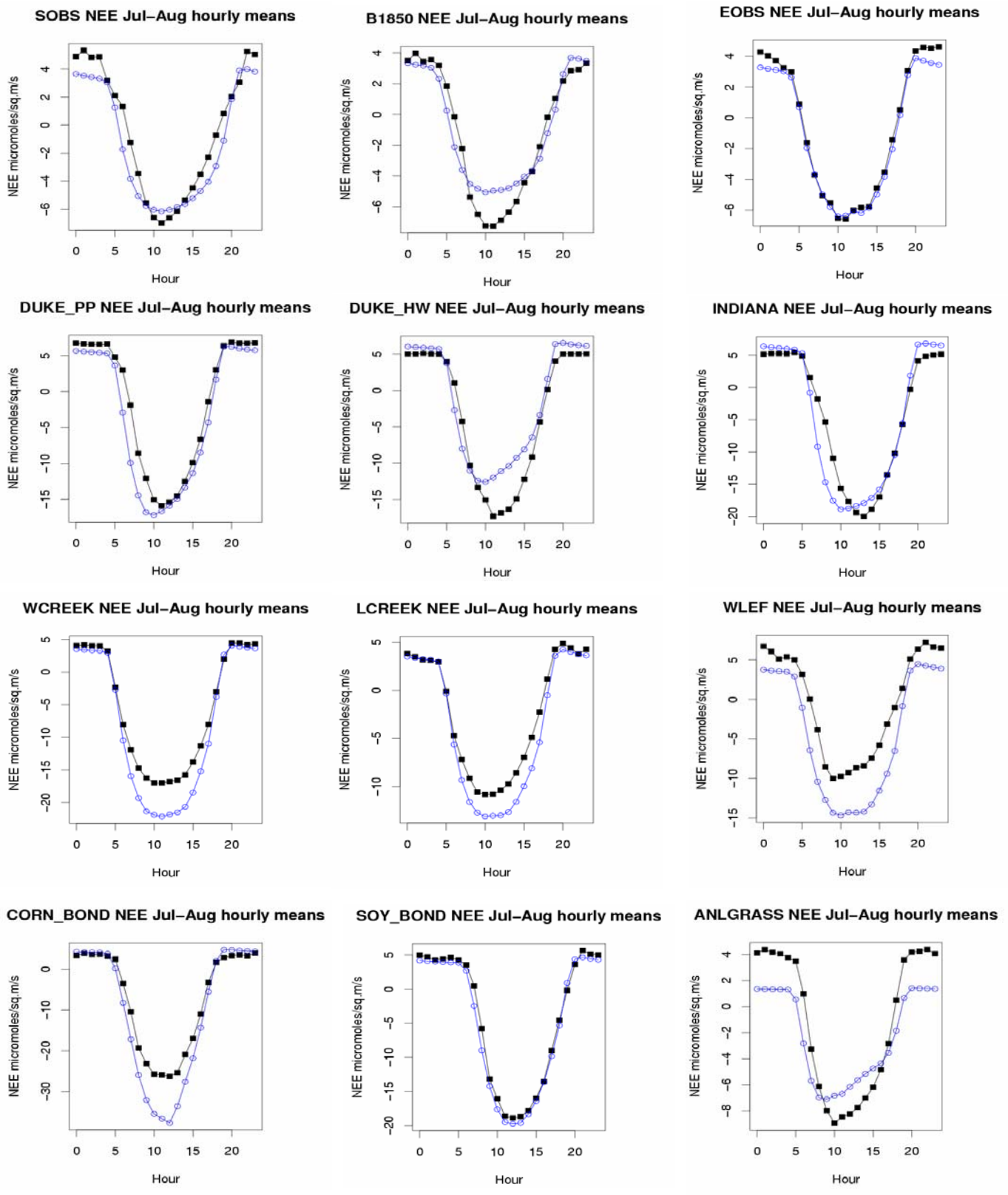


Figure 4: Comparison between the observed (solid-square) and predicted (open-circle) diurnal mean NEE (μmole $m^{-2}$ $s^{-1}$) over the peak photosynthetically active period, as in Fig. 2b, but at validation sites without adjustment of parameters.

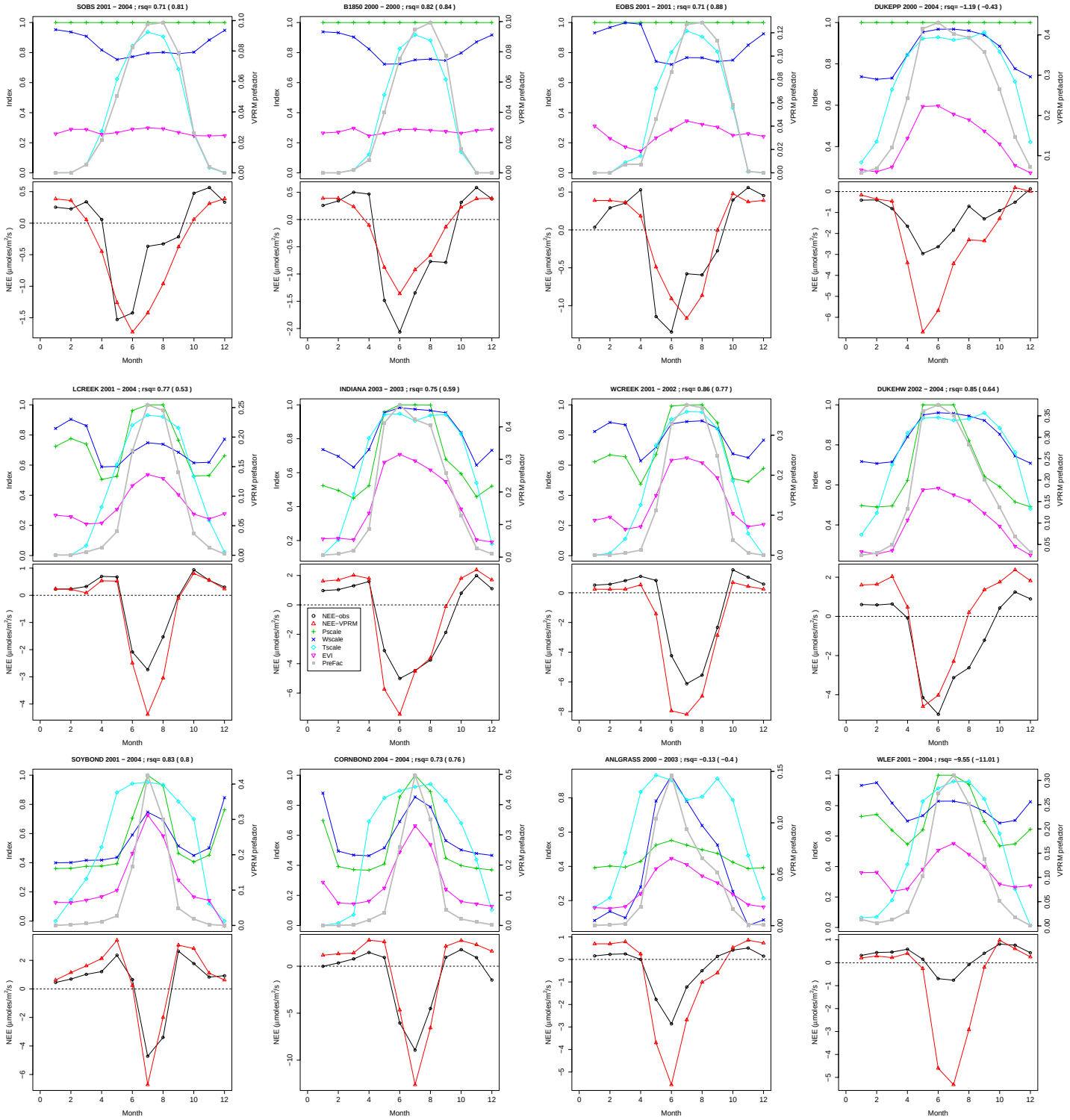


Figure 5: A comparison of the seasonal dynamics of model and observed NEE, as in Fig. 3, but at validation sites (no adjustment of VPRM parameters).

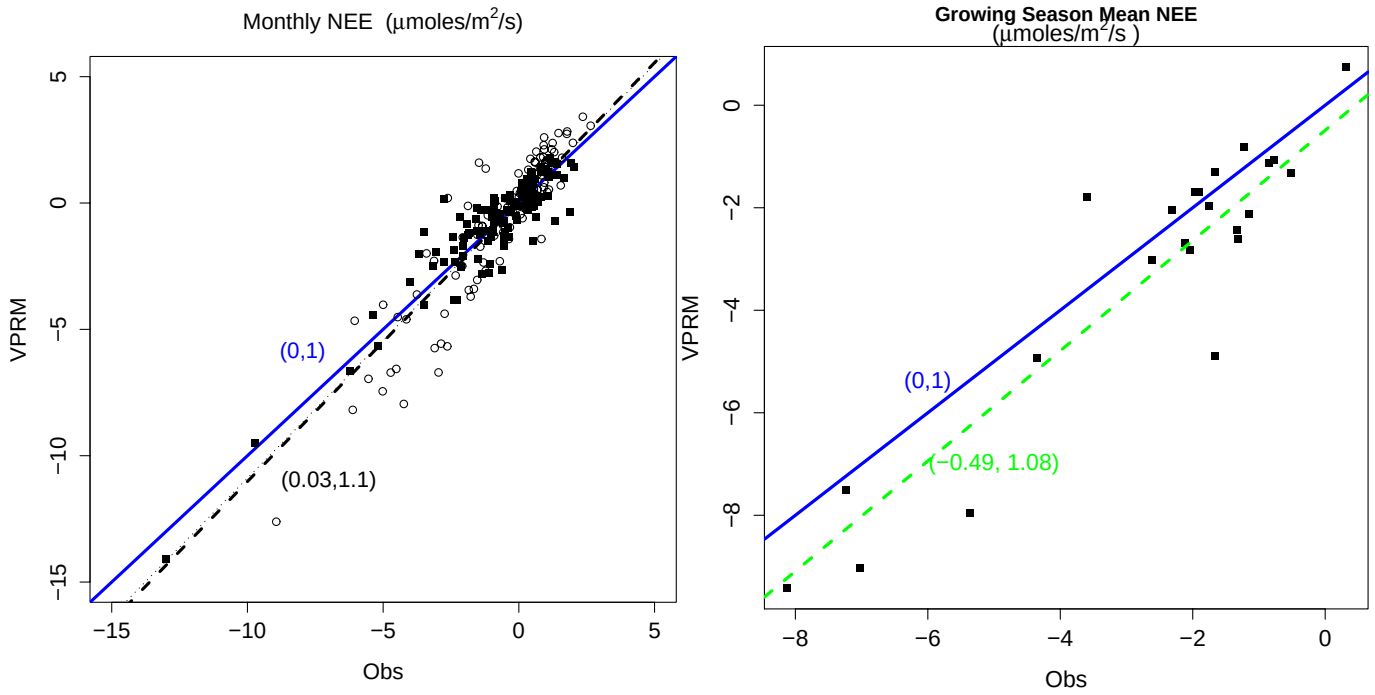


Figure 6: (*left* panel) Observed and predicted monthly mean NEE (µmole $m^{-2}$ $s^{-1}$) for calibration sites (solid symbols) and validation sites (open symbols) excluding WLEF. The regression line for all sites (dotted line) is very similar to the regression for validation sites only (dashed line). *(right panel*) Mean NEE by site (except WLEF) for the growing season.. The line labeled (0,1) has zero intercept and slope =1 ("1:1 line"). Regression lines are labeled similarly

a)

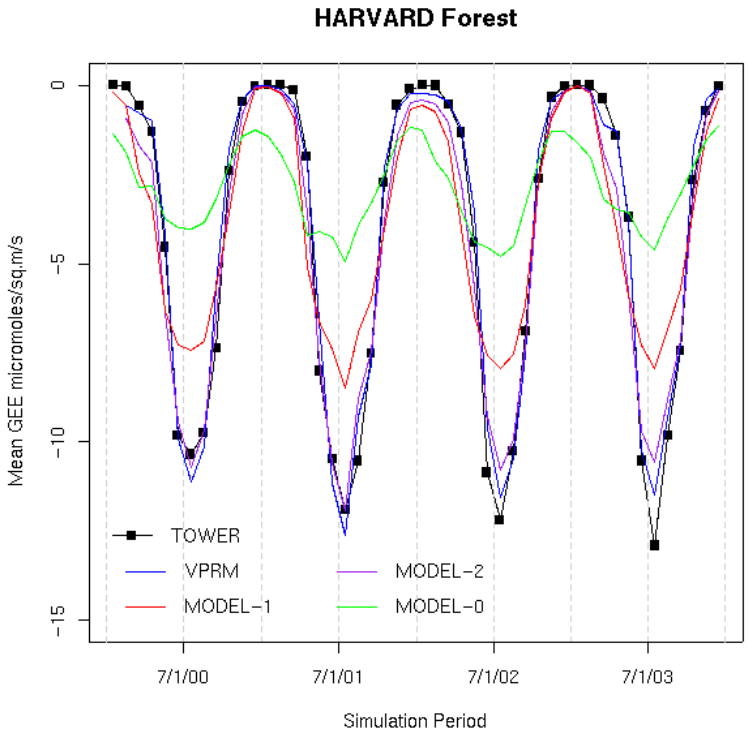


b)

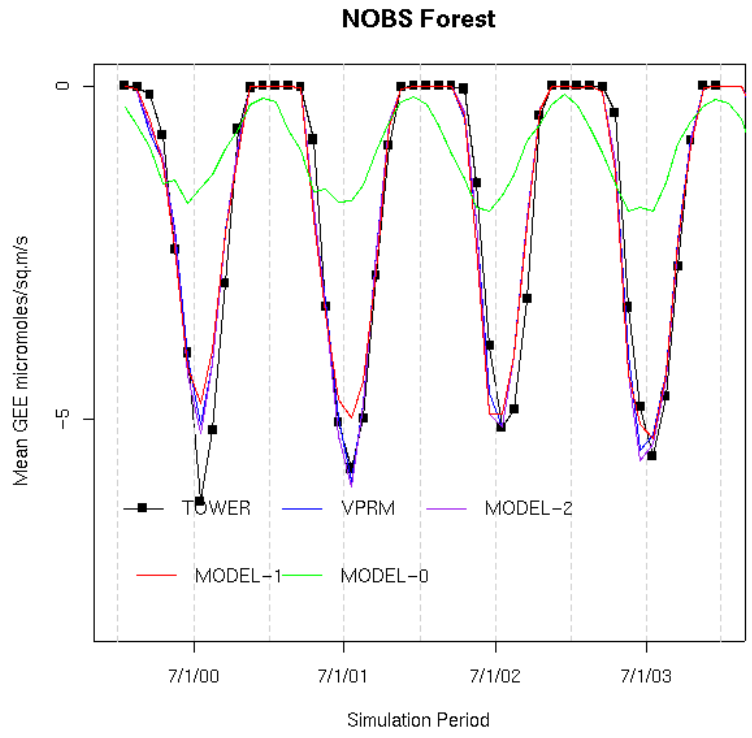


Figure 7a-b: A comparison between GEE (μmole $m^{-2}$ $s^{-2}$) obtained by fitting VPRM, MODEL-2, MODEL-1 and MODEL-0 to tower data from 2000 to 2003 at Harvard Forest. (*upper, 7a*) and NOBS/BOREAS (*upper, 7a*). The VPRM incorporates EVI, $P_{scale}$and $W_{scale}$ (driven by satellite data), plus $T_{scale}$ driven by meteorological data. MODEL-2 drops LSWI factors ($P_{scale}$and $W_{scale}$), MODEL-1 drops all satellite indices (EVI, $P_{scale}$and $W_{scale}$) and MODEL-0 drops all of these plus $T_{scale}$.